Tellus (1981), *33*, 597–603

A note on the mass flux for rapidly rotating recycling flow over topography

By JOHN E. HART, *Department of Astrogeophysics, University of Colorado, Boulder, Colorado 80309, U.S.A.*

(Manuscript received February 9, 1981)

ABSTRACT

This paper reports some measurements of the circumferential mass flux in a rotating cylindrical annulus spanned by a transverse ridge and containing a homogeneous liquid. Flows are driven by a differentially rotating lid in the shape of a parabola so as to simulate a polar β-plane. Unless the Rossby number $R_0 = \omega/2\Omega$, based on the lid rotation rate ω and the basic rotation rate Ω, is quite small the mass flux is less for the β-plane than for f-plane (flat lid) geometry. The mass flux is reduced in the β-plane case by mountain wave drag associated with the formation of Rossby waves in the annulus downstream of the topography. When R_0^2 is less than the Ekman number the β-plane mass flux exceeds that of the f-plane case. Streak photographs demonstrate the qualitative nature of the flow.

1. Introduction

Rapidly rotating recirculating flow over topography occurs in the Antarctic circumpolar current and in the Earth's atmosphere. These flows are of fundamental interest because they have the inherently non-linear property that the disturbance induced by the topography will alter the zonal flow incident on the topography via form-drag. Since the disturbance is itself generated by the zonal flow incident on the obstacle(s), a closed feedback loop is apparent. For a given external forcing that tends to accelerate a zonal flow, there will be a non-linear balance between the form-drag and the input torque. The nature of the balance depends crucially on the presence or absence of the variation of Coriolis parameter with latitude (the β effect). In some circumstances with strong β and very low friction, idealized analytical models of barotropic quasi-geostrophic flow over topography (Charney and DeVore, 1979; Hart, 1979) have indicated that this non-linear feedback between the topographically generated waves and the zonally averaged flow can lead to the appearance of multiple solutions. In other words, more than one steady-state flow is possible for fixed external parameters. This is one consequence of including zonal influence (the finite amplitude effect of mountain form-drag on the incident zonal flow) in the theory of large-scale disturbances induced by topography. Another consequence is that the circumferential mass flux generated in response to the driving is a strong function of β and of the driving itself. Such is not the case in models that treat a mountain-induced disturbance as isolated, with a pre-specified and fixed incident upstream flow (e.g. Hogg, 1973).

Hart (1977) and Davey (1978) showed that zonal influence would exist in a cyclic geometry provided only that the viscosity not vanish identically. In the limit of small viscosity there still can be an order one effect on the zonal flow due to the small phase shifts introduced on the mountain disturbance by friction. This point was emphasized by Maxworthy (1977) who gave experimental evidence of the strong dependence of circumferential mass flux on external (driving) Rossby number for an f-plane geometry. It is the purpose of this note to present experimental data on the circumferential mass flux in a rotating annulus driven by a parabolic differentially rotating lid, with bottom topography consisting of a hemispherical ridge spanning the gap. It is shown that the mass flux is very different when β is non-zero and the

 0040-2826/81/060597-07$02.50/0

driving is in the same sense as the basic rotation, than when an f- plane geometry or counter-rotating driving is used. This relates to the presence of strong Rossby wave drag in the former case. A simple theory that explains the data quite well for small to moderate Rossby numbers is presented.

2. Experimental results

Figs. 1 and 2 show a plan view and cross-section of the experimental apparatus. The fluid is contained in a cylinder that rotates at a basic rate Ω. Motion is driven by a contact lid that rotates differentially at rate ω. Thus the external Rossby number is

$$R_0 = \frac{\omega}{2\Omega}.$$

The upper lid was either flat, to simulate f-plane motions as in Maxworthy (1977), or parabolic, to simulate flow on a polar β-plane. The use of varying topography to mimic the variation of Coriolis parameter with latitude has often been used in laboratory analogues of geophysical flows (e.g. Beardsley, 1969).

The cylindrical annulus had an inner radius $R_i = 3$ cm and an outer radius $R_c = 23$ cm. The depth at the inner radius $H_0 = 11.0$ cm. For most runs $H_t = 2$ cm and the bottom topography was constructed of a glass cylindrical lens of height $H_m = 1.3$ cm, width $L = 5.6$ cm, and radius of curvature 3.6 cm. The basic rotation rate was maintained by a

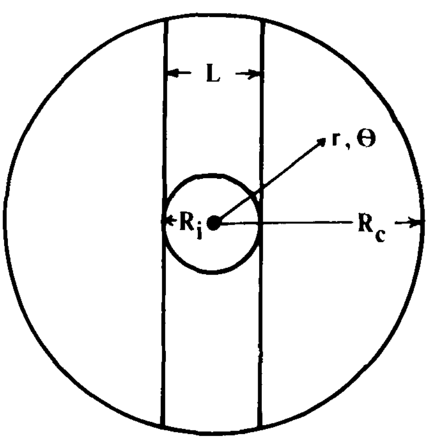

Fig. 1. Plan view of the experimental geometry.

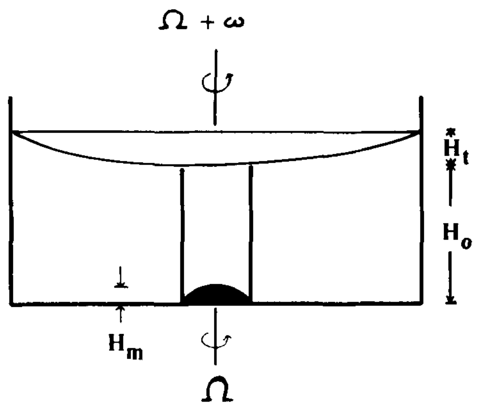

Fig. 2. Cross-section of the experimental geometry taken perpendicular to the axis of the transverse ridge.

servo-controlled motor, and the differential rotation by a synchronous motor driven by an audio oscillator.

First some streak photographs were taken to gain an overall impression of the flow structure. Neutrally buoyant floats were inserted and the system spun up to a final state. A horizontal sheet of light was passed through the plexiglass sidewalls at mid-depth and time exposures were made from above with a corotating camera. Fig. 3 shows the typical behavior. A slight part of the view is obstructed by the ω-drive support. The position of the transverse ridge is determined by the two white end markers near the walls. The dimensionless parameters represent the effect of β, (H_t/H_0), and friction (Ekman number $E = \nu/2\Omega H_0^2$). Rotation is anti-clockwise except for case (b) that is clockwise. For the flat top (a) an anticyclonic (opposite to the basic cyclonic or counterclockwise rotation of the apparatus) mountain vortex forms slightly upstream of the bump and the azimuthal flow is decreased near the outer wall. Since the flow is geostrophic the anti-cyclonic vortex implies a high pressure on the upstream slope so there will be a decelleration of the circumferential flow. For westward driving on the β-plane, Fig. 3(b), the flow over the ridge tends to be along lines of constant depth; fluid columns move radially outward as they go up over the bump, as opposed to the behaviour in Fig. 3(a) for the flat top. With eastward driving (Fig. 3(c), (d)) a set of stationary Rossby waves form in the lee. The amplitude and phase of these waves depend on the zonal circulation. The form drag associated with the waves in the presence of

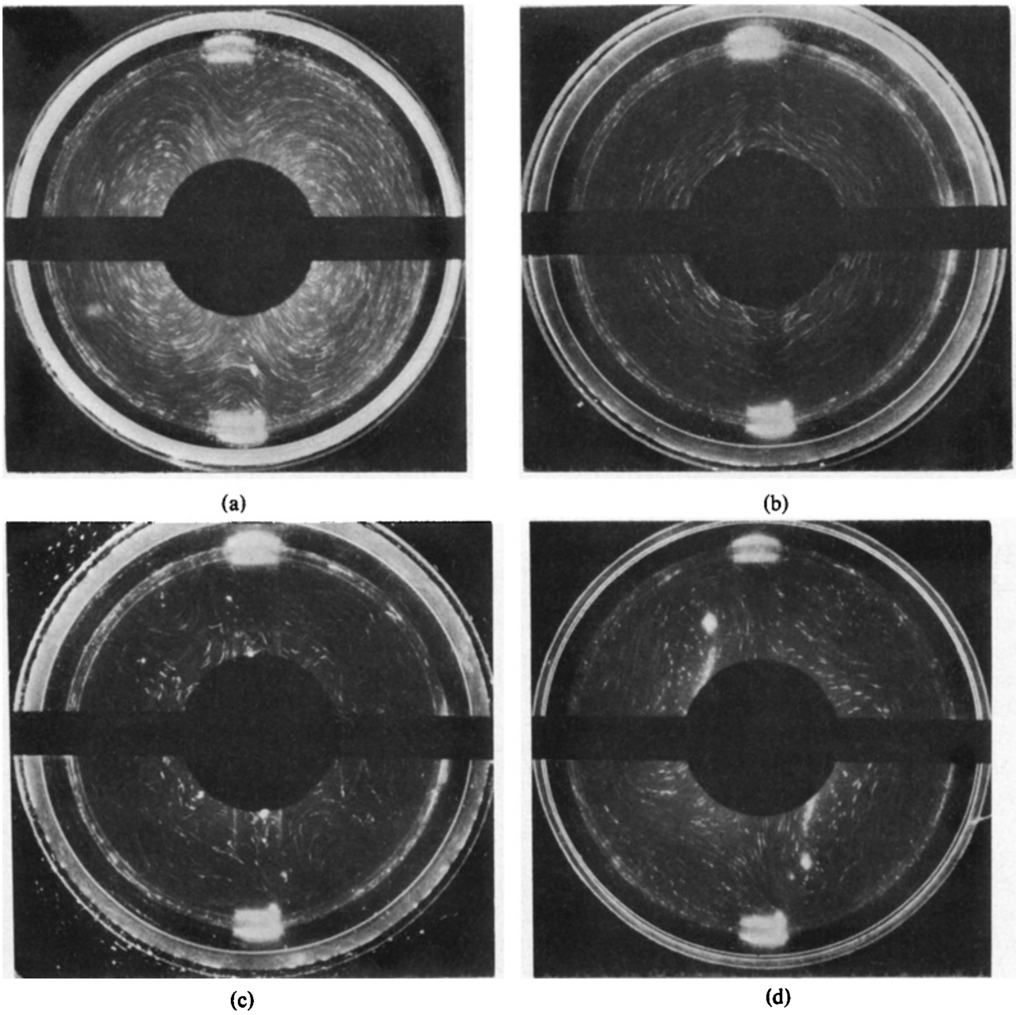

Fig. 3. Streak photographs for: (a) $H_t = 0$, $E = 0.0000086$, $R_0 = 0.021$; (b) $H_t/H_0 = 0.34$, $E = 0.000012$, $R_0 = -0.023$; (c) $H_t/H_0 = 0.34$, $E = 0.0000072$, $R_0 = 0.042$; (d) $H_t/H_0 = 0.18$, $E = 0.0000072$, $R_0 = 0.041$.

small friction is large, as is the zonal influence. As shown below, their presence has a very strong effect on the circumferential mass flux, being qualitatively different from what happens in the f-plane case characterized by Fig. 3(a).

The mass flux was measured by photographing dye streaks induced along a radial dye wire 29° downstream from the ridge and at mid-depth. The thymol blue dye technique of Baker (1966) was used. Fig. 4 shows a typical dye profile. The mass flux is the volume integral between the dye line and dye wire from top to bottom (since the flow is depth independent to order R_0), divided by the time interval between the dye initiation and the photograph. The dimensional flux is normalized by the flux M_0 of pure axisymmetric flow in the absence of topography but including $E^{1/4}$ sidewall layers at R_i and R_c. Formally

$$M^* = \int_{R_i}^{R_c} hv \, dr$$

where v is the azimuthal velocity. M_0 is obtained from a similar integration except that v is replaced by $\hat{v}$, the velocity in purely axisymmetric flow.

Fig. 5 shows the mass flux data. Included is the

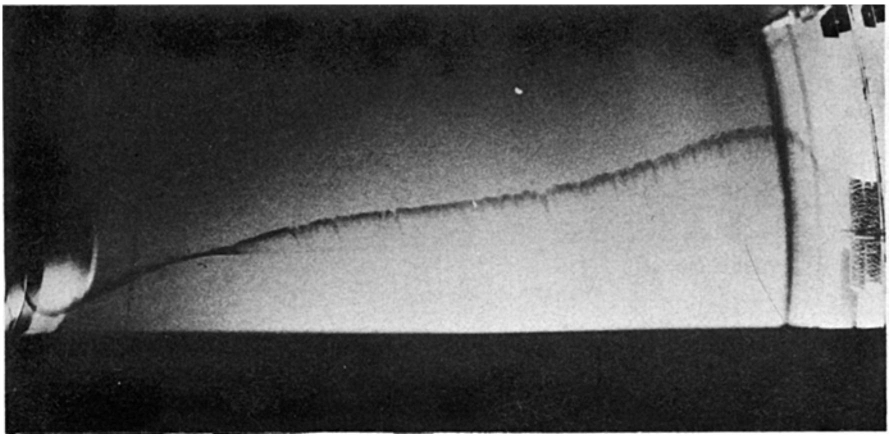

Fig. 4. Typical thymol dye trace used to get M. $E = 0.000012$, $R_0 = 0.0074$, $H_t/H_0 = 0.18$, $H_m/H_0 = 0.116$

predicted mass flux from the theory outlined in Section 3 for the flow on the β-plane. As anticipated there is a substantial difference between the flat lid and parabolic lid cases. For the former the mass flux increases almost monotonically with R_0. This is in agreement with the findings of Maxworthy who measured M/M_0 for flow over a single transverse ridge on an f-plane. In this case when R_0 approaches zero the flow is entirely blocked except for thin viscous regions near the walls because there are no circumferential depth contours. As R_0 increases more and more fluid can be carried over the ridges by inertial effects. Thus the mass flux grows with R_0.

The β-plane case is entirely different. M/M_0 decreases rapidly with increasing R_0 near $R_0 = 0$. At $R_0 = 0$ there is a non-zero flux because there exists a large number of circumferential depth contours on which the fluid can move around the annulus. This is partly a result of having H_m/H_t of order one. When R_0 is negative there is a horizontally trapped disturbance over the mountain. There are no Rossby waves, as their phase speeds are in the same direction as the zonal component of the flow. The disturbance has an amplitude that represents a balance between topographic stretching and horizontal advection. As $-R_0$ increases the perturbation weakens and M/M_0 increases. As R_0 increases to moderate positive values, larger and larger stationary Rossby waves are excited. The form drag associated with these waves causes the mass flux to fall rapidly.

For Rossby numbers larger than those presented in Fig. 5, the flow velocities become too fast for effective use of the thymol technique.

3. A simple theoretical model

We present a simple model for the β-plane flow described above and compare its mass flux prediction with experiment. To be precise we specify the bottom topography non-dimensionally by

$$h^* = H_m h_m(r^*, \theta) \tag{1}$$

that in our case intersects both the inner and outer boundaries. The top lid is at

$$h^* = H_0\left(1 + \frac{H_t r^{*2}}{2H_0 R_c^2}\right) \tag{2}$$

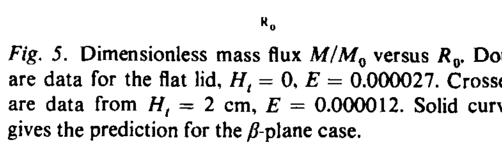

Fig. 5. Dimensionless mass flux M/M_0 versus R_0. Dots are data for the flat lid, $H_t = 0$, $E = 0.000027$. Crosses are data from $H_t = 2$ cm, $E = 0.000012$. Solid curve gives the prediction for the β-plane case.

where H_t is the magnitude of the lid variation, r^* the dimensional radius, θ the polar angle, and R_c the outer radius of the cylinder. H_0 is the reference depth and is assumed to be much greater than either H_t or the topography height scale H_m. Since the lid rotates differentially at rate ω, we introduce a time scale ω^{-1}, a velocity scale ωR_c, and a length scale R_c. Then the appropriate one-layer quasi-geostrophic vorticity equation valid for small R_0 is

$$\frac{\partial}{\partial t}\nabla^2\psi + J\left(\psi, \nabla^2\psi + \frac{H_m h_m}{R_0 H_o} - \frac{H_t r^2}{2R_0 H_0}\right) = \frac{\sqrt{2}\,E^{1/2}}{R_0}(1-\nabla^2\psi) \tag{3}$$

where ψ is the stream function for the depth invariant interior velocity such that

$$v = \frac{\partial\psi}{\partial r}$$

$$u = -\frac{1}{r}\frac{\partial\psi}{\partial\theta}.$$

The last term in (3) represents the effects of Ekman suction derived from the differentially rotating lid, and from internal vorticity. Thus we retain bottom friction but neglect sidewall friction in this theoretical model. Such is the case in most previous work. It is useful to note that a parabolic lid leads to a linear Rossby wave phase speed that is independent of radius, while a conical lid does not.

Consider steady solutions of (3) in an annulus with walls at R_i and R_c. Since we have neglected lateral friction, the boundary conditions we can impose are the inviscid ones

$$\psi\left(r = \frac{R_i}{R_c}, \theta\right) = 0 \qquad . \tag{4}$$

$$\psi(r = 1, \theta) = M,$$

where M is undetermined as yet. Since $M = \int_{R_i/R_c}^{1} v\, dr$, it is essentially the non-dimensional circumferential mass flux, and is precisely the quantity we wish to predict as a function of external conditions.

By averaging eq. (3) zonally over θ, then integrating once $\int^r r\, dr$, and once across the annulus, it is possible to show that

$$\frac{\sqrt{2}E^{1/2}H_0}{H_m}(M - \tfrac{1}{4}) = +\int_{R_i/R_c}^{1}\left\{\overline{\frac{1}{r}\frac{\partial\psi}{\partial\theta}h_m} + \frac{H_0 R_0}{H_m r^2}\overline{\frac{\partial\psi}{\partial\theta}\frac{\partial rv}{\partial r}}\right\}dr \tag{5}$$

with the overbar denoting a zonal average $1/\pi \int_0^\pi d\theta$. The first term on the right-hand side of this equation represents direct form drag on the obstacle, while the second reflects a redistribution of zonal circulation by the mountain-induced θ-dependent flow. Clearly if there is no topography the mass flux is just $M_0 = 0.25$, but if $h_m \neq 0$ there is an average effect of the obstacle on the zonal flow and on the mass flux. As shown by Hart (1977), the terms on the right-hand side of (5) are proportional to $E^{1/2}$, so for both small and large friction one expects a substantial zonal influence. In the case where the mountains vary much more rapidly in θ than in r, the second term on the right-hand side of (7) is negligible (Hart, 1979).

A crude but informative theory can be constructed by assuming that the zonally averaged azimuthal flow has the form $\bar{v} = Ar$, where A is a constant not necessarily equal to $\tfrac{1}{2}$. This approximation is valid in the limit of small amplitude waves $H_m/H_0 \ll R_0$, and is also accurate for large amplitude waves when the topography and flow are in the form of long narrow ridges. The experimental configuration does not exactly correspond to this latter condition, but the aspect ratio of the topography is moderately small.[1] We represent the stream function as a mean azimuthal flow plus a finite amplitude disturbance, $\psi = \tfrac{1}{2}Ar^2 + \phi(r,\theta)$. Neglecting all wave–wave interactions (also valid in the narrow ridge limit), the disturbance field is governed by the quasi-linear equation

$$\frac{\partial}{\partial\theta}\left[A\nabla^2\phi + \frac{H_t\phi}{R_0 H_0}\right] + \frac{\sqrt{2}E^{1/2}}{R_0}\nabla^2\phi = -\frac{AH_m}{R_0 H_0}\frac{\partial h_m}{\partial\theta}. \tag{6}$$

[1] Since the limit of large R_0 is not attained experimentally, we expect this crude theory to work best near $R_0 = 0$ since then the Rossby waves that form in the lee of the mountains have short downstream wavelengths and relatively slow radial variation.

In the anisotropic limit where $1/r(\partial/\partial\theta) \gg \partial/\partial r$ eq. (5) becomes

$$A - \tfrac{1}{2} = \frac{\sqrt{2}H_m}{E^{1/2}H_0}\int_{R_i/R_c}^{1} \overline{\frac{1}{r}\frac{\partial\phi}{\partial\theta} h_m}\, dr. \qquad (7)$$

Since in our experiments $R_j/R_c = 0.13$ the lower limits in the integrals of eq. (9) can be set equal to zero without major error.

Note that once $h_m(r,\theta)$ is specified, eqs. (6) and (7) form a closed problem. In the experiments the topography is generated by attaching a cylindrical section to the bottom of the tank (see Section 2). The topography can be represented by a Fourier–Bessel series

$$h_m = \sum_{\substack{k \\ n(\text{even})}} h_{kn} J_n(l_{kn} r) \cos n\theta$$

where

$$\hat{h}_{kn} = 4 \int_0^1 r J_n(l_{kn} r)\, dr \times \int_0^{\theta_h(r)} h(r,\theta) \cos n\theta \, d\theta / J_{n-1}^2(l_{kn})$$

with

$$\theta_h = \sin^{-1}(L/2rR_c).$$

Solutions to (6) can be found with the form

$$\phi = \sum_{\substack{k \\ n}} \phi_{kn} e^{in\theta} J_n(l_{kn} r)$$

where $J_n(l_{kn}) = 0$. ϕ_{kn} is a function of m, n, A, and the external parameters. Substituting this solution into (7) and evaluating all the interaction and topography integrals (numerically) yields an algebraic equation for A. It is

$$\frac{A - \tfrac{1}{2}}{A} = -\frac{H_m^2}{H_0^2} \times \sum_{\substack{k \\ n(\text{even})}} \frac{n^2 Q_{kn}}{l_{kn}^2 [E + n^2(R_0 A - H_t/H_0\, l_{kn}^2)^2]} \qquad (8)$$

where Q_{mn} contains the interaction integrals that depend on the details of the topography but not on the external parameters. The right-hand side of this equation reflects the Rossby wave drag. It peaks at each linear inviscid wave resonance when E is very small. However at small R_0 the peaks are obscured because Q_{kn} is small when k and n are large.

Equation (8) is easily solved for A, and hence M/M_0 can be predicted. The results corresponding to the experimental conditions are shown as a solid curve in Fig. 5. There is good qualitative agreement between theory and experiment for most values of R_0, considering the approximations involved in the theory. This agreement reconfirms our interpretation that Rossby waves generated by the topography are responsible for the large zonal influence. At larger R_0, above 0.033, the theory predicts multiple equilibria where more than one value of M/M_0 is indicated for the same external conditions. Such multiple states were not observed by the thymol technique when hysteresis experiments were done. However this range of R_0 corresponds to regions of parameter space where the assumption of anisotropic disturbances is not at all well satisfied, so that wave–wave interactions, radially varying zonal flows, and the second term on the right-hand side of (5) should all be included. All this would require a complete numerical solution of the governing quasi-geostrophic vorticity equation. Such a solution might not predict these multiple solutions.

4. Conclusions

We have given experimental and theoretical evidence that the zonal influence for rapidly rotating flow over topography on a β-plane becomes very small for negative driving Rossby number R_0, and quite large for positive R_0 when Rossby waves are excited in the lee. The negative R_0 behavior is a consequence of having only a weak horizontally trapped topographic disturbance with a very small downstream shift of the vortex off the crest for R_0 less than about −0.005. When the topographic β-effect and vortex stretching due to the obstacle are comparable ($H_m \sim H_t$) the circumferential mass flux is much larger at small R_0 than when H_m/H_t is very large (f-plane) because of the existence of cyclic depth contours in the former instance.

5. Acknowledgement

This research was supported by the National Science Foundation through grant NSF-ATM-76-17028 to the University of Colorado.

REFERENCES

Baker, D. J. 1966. A technique for the precise measurement of small fluid velocities. *J. Fluid Mech. 26*, 573–576.

Beardsley, R. C. 1969. A laboratory model of the wind-driven ocean circulation. *J. Fluid Mech. 38*, 255–272.

Charney, J. G. and DeVore, J. 1979. Multiple flow equilibria in the atmosphere and blocking. *J. Atmos. Sci. 36*, 1205–1216.

Davey, M. K. 1978. Recycling flow over bottom topography in a rotating annulus. *J. Fluid Mech. 87*, 497–520.

Hart, J. E. 1977. A note on quasi-geostrophic flow over topography in bounded basins. *J. Fluid Mech. 79*, 657–668.

Hart, J. E. 1979. Barotropic quasi-geostrophic flow over anisotropic mountains. *J. Atmos. Sci. 36*, 1736–1746.

Hogg, N. G. 1973. On the stratified Taylor column. *J. Fluid Mech. 58*, 517–537.

Maxworthy, T. 1977. Topographic effects in rapidly-rotating fluids: Flow over a transverse ridge. *J. Appl. Math. and Phys. (ZAMP) 28*, 853–863.

ЗАМЕЧАНИЕ О ПОТОКЕ МАССЫ ДЛЯ БЫСТРО ВРАЩЕГОСЯ КРУГОВГО ПОТОКА НАД ТОПОГРАФИЕЙ

В статье сообщаются результаты некоторых измерений замкнутого кругового потока массы во вращающемся цилиндрическом кольцевом сосуде с радиальным хребтом, содержащим однородную жидкость. Течение возбуждается дифференциально вращающейся крышкой, имеющей форму параболы в поперечном сечении, моделирующей полярную –плоскость. Пока число Россби $R = 2$, основанное на скорости вращения крышки и скорости вращения сосуда , мало, поток массы меньше для геометрии –плоскости, чем для f–плоскости (плоская крышка). Поток массы в случае –пцоскости уменьмается из-за волнового сопротивления гор, связанного с образованием волн Россбм в сосуде вниз по течению от хребта. Когда R менрше числа Экмана, поток массы в случае –плоскости превымает таковой для случая f–плоскости. Фотографии треков частиц демонстрируют качественную природу течений.